Geophysical Research Letters

RESEARCH LETTER
10.1029/2024GL109090

Cloud Radiative Effects Associated With Daily Weather Regimes

Ming Zhao[1]

[1]Geophysical Fluid Dynamics Laboratory National Oceanic and Atmospheric Administration, Princeton, NJ, USA

Key Points:

- Cloud radiative effect (CRE) associated with various daily weather regimes including atmospheric rivers (ARs), tropical storms (TSs), and mesoscale convection systems (MCSs) are derived using satellite observations and reanalysis data
- Precipitation (wet) days account for roughly 80% (60%) of global longwave (LW) and shortwave (SW) CRE due to their large frequency and high intensity in CRE
- Despite their rare occurrence, AR, TS, and MCS days together account for 32% of LW CRE and 27% of SW CRE due to their higher intensity CRE

Supporting Information:

Supporting Information may be found in the online version of this article.

Correspondence to:

M. Zhao,
ming.zhao@noaa.gov

Citation:

Zhao, M. (2024). Cloud radiative effects associated with daily weather regimes. *Geophysical Research Letters*, *51*, e2024GL109090. https://doi.org/10.1029/2024GL109090

Received 8 MAR 2024
Accepted 27 APR 2024

Author Contribution:

Conceptualization: Ming Zhao
Data curation: Ming Zhao
Formal analysis: Ming Zhao
Investigation: Ming Zhao
Methodology: Ming Zhao
Project administration: Ming Zhao
Resources: Ming Zhao
Software: Ming Zhao
Supervision: Ming Zhao
Validation: Ming Zhao
Visualization: Ming Zhao

Abstract Using high temporal resolution satellite observations and reanalysis data, we classify daily weather into distinct regimes and quantify their associated cloud radiative effect (CRE) to better understand the roles of various weather systems in affecting Earth's top-of-atmosphere radiation budget. These regimes include non-precipitation, drizzle, wet non-storm, and storm days, which encompass atmospheric rivers (AR), tropical storms (TS), and mesoscale convection systems (MCS). We find that precipitation (wet) days account for roughly 80% (60%) of global longwave (LW) and shortwave (SW) CREs due to their large frequency and high intensity in CRE. Despite being rare globally (13%), AR, TS, and MCS days together account for 32% of global LW CRE and 27% of SW CRE due to their higher intensity in LW and SW CRE. These results enhance our understanding of how various weather systems, particularly severe storms, influence Earth's radiative balance, and will help to better constrain climate models.

Plain Language Summary Using detailed satellite observations and reanalysis data, we categorize daily weather patterns into different types and measure the cloud radiative effects (CRE) associated with each type. The weather patterns we study include non-precipitation days, drizzle, wet non-storm days, and storm days, which include events like atmospheric rivers, tropical storms, and mesoscale convective systems. We found that precipitation days, which include both drizzle and wet days, contribute to about 80% of global longwave (LW) and shortwave (SW) CRE due to their high frequency and intensity. Even though storm days are rare globally (only 13%), they collectively contribute to around 32% of global LW CRE and 27% of SW CRE because of their stronger impact on both LW and SW CRE. These findings are important for understanding how different weather systems influence the Earth's radiation balance and will help improve the accuracy of climate models.

1. Introduction

Clouds cover about two-thirds of the Earth's surface and are often organized into coherent systems by large-scale atmospheric flows. They can either warm the Earth by trapping outgoing longwave (LW) radiation (OLR) or cool it by reflecting shortwave (SW) solar radiation back to space. The net effect depends on factors such as cloud height, type, and optical properties. The impact of clouds on the Earth's top-of-atmosphere (TOA) radiation budget, known as cloud radiative effect (CRE), can be deduced from satellite observations comparing upwelling radiation in cloudy and non-cloudy regions. Globally, the annual mean LW and SW CRE are roughly 30 and -50 W m^{-2} respectively, resulting in a net CRE of about -20 W m^{-2} in the present climate, implying a net cooling effect from clouds. Given the large magnitude of CRE, clouds have the potential to significantly influence climate feedback. Indeed, cloud feedback has been identified as the primary source of uncertainties in climate models' projections of future climate since the first IPCC assessment report (Cess et al., 1990; Flato et al., 2013; Meehl et al., 2007; Randall et al., 2007; Soden & Held, 2006; Zhao, 2014, 2022a; Zhao et al., 2016). Unfortunately, a reliable observational constraint on global cloud feedback remains elusive due to the short satellite record as well as other complexities.

To narrow down cloud feedback uncertainty and improve climate models' fidelity in future projections, it would be natural to focus on reducing model biases in simulations of the observed present-day CRE. Climate model developments often tune present-day CRE toward observed long-term mean climatology (Danabasoglu et al., 2020; Donner et al., 2011; Golaz et al., 2019; Held et al., 2019; Zhao et al., 2018). However, models with similar climatological CRE can still differ substantially due to compensating errors among various weather regimes. These differences could lead to varying cloud feedback as weather regime statistics change in warmer climates. Thus, adding observational constraints to modeled CRE based on individual weather regimes is crucial.

Writing – original draft: Ming Zhao
Writing – review & editing: Ming Zhao

Earlier studies focused on cloud regimes classified by the radiative properties of clouds (Oreopoulos et al., 2016). Many studies also emphasize fair-weather cumuli and stratocumulus clouds, which typically exhibit little surface precipitation but have either large spatial coverage (shallow cumuli) or strong net CRE (stratocumulus), making them important contributors to the global radiative budget (Bony & Dufresne, 2005; Bony et al., 2004; Bretherton, 2015; Yuan et al., 2018). In comparison, the CRE associated with precipitating clouds, particularly those generated by high-impact severe storms, has received less attention regarding their contributions to the global TOA radiative budget presumably due to their relatively rare occurrence.

In this study, we aim to quantify the CRE associated with atmospheric rivers (AR), tropical storms (TS), and mesoscale convection systems (MCS)—collectively referred to as storms here—in addition to other daily weather regimes such as non-precipitating, drizzle, and wet non-storm days (i.e., days that are wet but not AR, TS, or MCS). Zhao (2022b) demonstrated that despite their rare occurrence globally (~13%), these organized storm systems collectively account for more than 50% of global and annual mean precipitation and ~75% of extreme precipitation, with daily rate exceeding the local 99th percentile of daily precipitation. However, their contribution to the global and annual mean TOA radiation has not yet been estimated in the literature. Here, we utilize high-temporal-resolution satellite observations and reanalysis data to estimate the TOA CREs associated with these high-impact weather events. In doing so, we also attempt to assess the CRE associated with other daily weather regimes characterized by significant surface precipitation, such as drizzle and wet non-storm days. The results will be useful for understanding the roles of various weather systems in Earth's radiative budget and for more in-depth climate model evaluations. Below Section 2 describes the observational data and analysis methods. Section 3 presents the results. Section 4 provides a summary and discussion.

2. Data and Methods

We utilize the synoptic TOA and surface fluxes, and clouds data set (SYN1deg-Ed4.1—Level 3) at 1° × 1° resolution from the Clouds and the Earth's Radiant Energy System (CERES) (Smith et al., 2011), accessible at https://ceres.larc.nasa.gov/data/, to derive daily LW and SW CRE for the period of 2001–2020. It's important to note that the long-term global and monthly mean values of TOA radiative fluxes from CERES-SYN1deg-Ed4.1 are not identical to those from the CERES Energy Balanced and Filled data (CERES-EBAF-Ed4.1) (Loeb et al., 2009), which are routinely used for evaluating global climate models at monthly or longer time scales. To facilitate comparisons with climate model simulations in the future, the small difference in the long-term (2001–2020) global and monthly mean values of TOA fluxes between CERES-SYN1deg-Ed4.1 and CERES-EBAF-Ed4.1 is added to the CERES-SYN1deg-Ed4.1 data as a global constant for each month. This adjustment ensures that the corrected CERES-SYN1deg-Ed4.1 data produce identical global and monthly mean values of TOA fluxes as CERES-EBAF4.1-Ed4.1. This small adjustment does not significantly affect our results and conclusions.

To classify daily precipitation regimes, we utilize observed daily precipitation data from the Multi-Source Weighted-Ensemble Precipitation (MSWEP-v2) data set (Beck et al., 2019), which offers global coverage of precipitation at fine spatial and temporal resolutions. For detecting ARs, we employ 6-hourly vertically integrated vapor transport (IVT) data from the ERA-5 reanalysis (Hersbach et al., 2020). TS tracks are obtained from the International Best Track Archive for Climate Stewardship (IBTrACS) (Knapp et al., 2010), which provides global coverage of 6-hourly TS track data. To detect MCSs, we utilize the CLoud Archive User Service (CLAUS) multisatellite infrared brightness temperature data set (Hodges et al., 2000), which offers 3-hourly global coverage of brightness temperature (T_b) for the 1985–2008 period. Since the CLAUS data only cover the 1985–2008 period, whereas the CERES data start from 2001, we analyze the MCS-associated CRE for the period of 2001–2008, with the rest of the analysis covering the period of 2001–2020. All data are first regridded to a common grid before analysis.

The methods for detecting AR, TS, and MCS objects have been documented in (Dong et al., 2021; Guan & Waliser, 2015; Zhao, 2020, 2022b; Zhao et al., 2009). Following Zhao (2022b), for any given grid cells, if at least one AR/TS/MCS condition is identified from the 6-hourly data during a calendar day and the daily surface precipitation rate $P_{day} \geq 1$ mm day^{-1}, the day is subsequently identified as an AR/TS/MCS day. We also make the AR, TS, and MCS days mutually exclusive by setting a priority for each identified phenomenon. Specifically, for any given grid cell, if a day satisfies multiple conditions, it is first considered as a TS day, then an AR day, and finally an MCS day. This priority choice is partly due to our confidence level in detecting TS, AR, and MCS days.

Among the three phenomena, we have relatively lower confidence in detecting MCS; thus, we consider a day as an MCS day only when it is neither an AR nor a TS day. Below, we also refer to an AR, TS, or MCS day as a storm day.

In addition to the storm days, we define a wet day as a calendar day with a daily precipitation rate $P_{day} \geq 1$ mm day^{-1} so that an AR, TS, or MCS (i.e., storm) day must also be a wet day. We refer to a wet day that is not an AR, TS, or MCS day as a wet non-storm day. Furthermore, we define a precipitation (drizzle) day as a calendar day with a daily precipitation rate $P_{day} \geq 0.2$ mm day^{-1} (0.2 mm day^{-1} $\leq P_{day} < 1$ mm day^{-1}). Any calendar day with $P_{day} < 0.2$ mm day^{-1} is considered as a non-precipitation day (i.e., no significant measurable precipitation at the surface). Thus, for any given grid cells, a calendar day is classified into one of the following six categories: non-precipitation, drizzle, wet non-storm, AR, TS, or MCS days. Note that by definition, precipitation and non-precipitation days together encompass all calendar days. Drizzle and wet days combined constitute all precipitation days. Wet non-storm days and storm days collectively comprise all wet days. Finally, AR, TS, and MCS days collectively constitute all storm days. Using this classification, we conditionally sample the daily TOA radiation fluxes to explore the contribution of each daily weather regime to the global and regional mean TOA radiative budget as well as the CREs. Below, we present the results.

3. Results

We first illustrate in Figure 1 the annual occurrence frequency of the precipitation, drizzle, wet, AR, TS, MCS, storm (i.e., AR + TS + MCS), and wet non-storm days. Globally, the frequency of precipitation days is 62.5%, substantially larger than that of non-precipitation days (37.5%). Among the 62.5% precipitation days, 22.6% are drizzle days and 39.9% are wet days, with 27% classified as non-storm days and 13% as storm days. Furthermore, among the 13% storm days, approximately 8% are AR days, 4.2% are MCS days, and 0.72% are TS days. Thus, globally, storm days may be considered as rare events. Regionally, each type of storm days can occur more frequently, with most AR days occurring in the mid-latitudes, TS days in the subtropical tropical cyclone main development region, and MCS days in the deep tropics. Compared to storm days, wet non-storm days tend to be more widespread, with a higher occurrence frequency over the Inter-Tropical Convergence Zone (ITCZ), South Pacific Convergence Zone (SPCZ), equatorial Indian Ocean, northern edge of the mid-latitude storm track regions, as well as parts of tropical land. In contrast, drizzle days tend to occur more frequently over the eastern part of the Pacific, Atlantic, and South Indian Ocean basins, where there is a large coverage of stratocumulus clouds, with minimum occurrence in the ITCZ, SPCZ and equatorial Indian Ocean. The occurrence frequency of each daily precipitation regime is important for its contribution to the annual mean LW and SW CRE, as well as precipitation.

In Figure 2, we present the annual mean LW CRE and its contributions (i.e., the cumulative LW CRE over all event days) from drizzle, wet, AR, TS, MCS, storm, and wet non-storm days. The global mean values are shown at the top of each panel. Note that the combined contributions from drizzle and wet days represent the total LW CRE from all precipitation days, while the difference between the annual mean LW CRE and that from all precipitation days indicates the contributions from non-precipitation days. Both the global mean and spatial distribution of LW CRE are largely determined by precipitation days, especially wet days. However, storm days produce disproportionately larger global LW CRE. For instance, globally, although storm (AR + TS + MCS) days account for only about 13% of the total days, they contribute to 32% (i.e., 8.27/25.84) of the global LW CRE. This contribution is close to that produced by all wet non-storm days, which occur about twice as frequently as storm days. Individually, the global and annual mean LW CRE associated with AR, TS, and MCS days are 3.92 W m^{-2} (15.2%), 0.54 W m^{-2} (2.1%), and 3.77 W m^{-2} (14.6%), respectively. Regionally, the percentage contribution to LW CRE from AR, TS, and MCS days can be substantially larger (40%–50%) over regions such as the ITCZ, the SPCZ, and the mid-latitude storm track regions, with AR dominating in the mid-latitudes and MCS days in the tropics. Thus, these severe storms are important contributors to TOA LW CRE both globally and regionally. Storm days and wet non-storm days (i.e., wet days) together account for approximately 67% of the global TOA LW CRE. If we further include the drizzle days, the total contribution from all precipitation days amounts to approximately 83% of the global LW CRE.

The geographical distribution of LW CRE (i.e., the mean LW CRE intensity of an event day) averaged from non-precipitation, drizzle, wet, AR, TS, MCS, storm, and wet non-storm days is shown in Figure S1 of Supporting Information S1. As expected, LW CRE generally increases with surface precipitation at a given location.

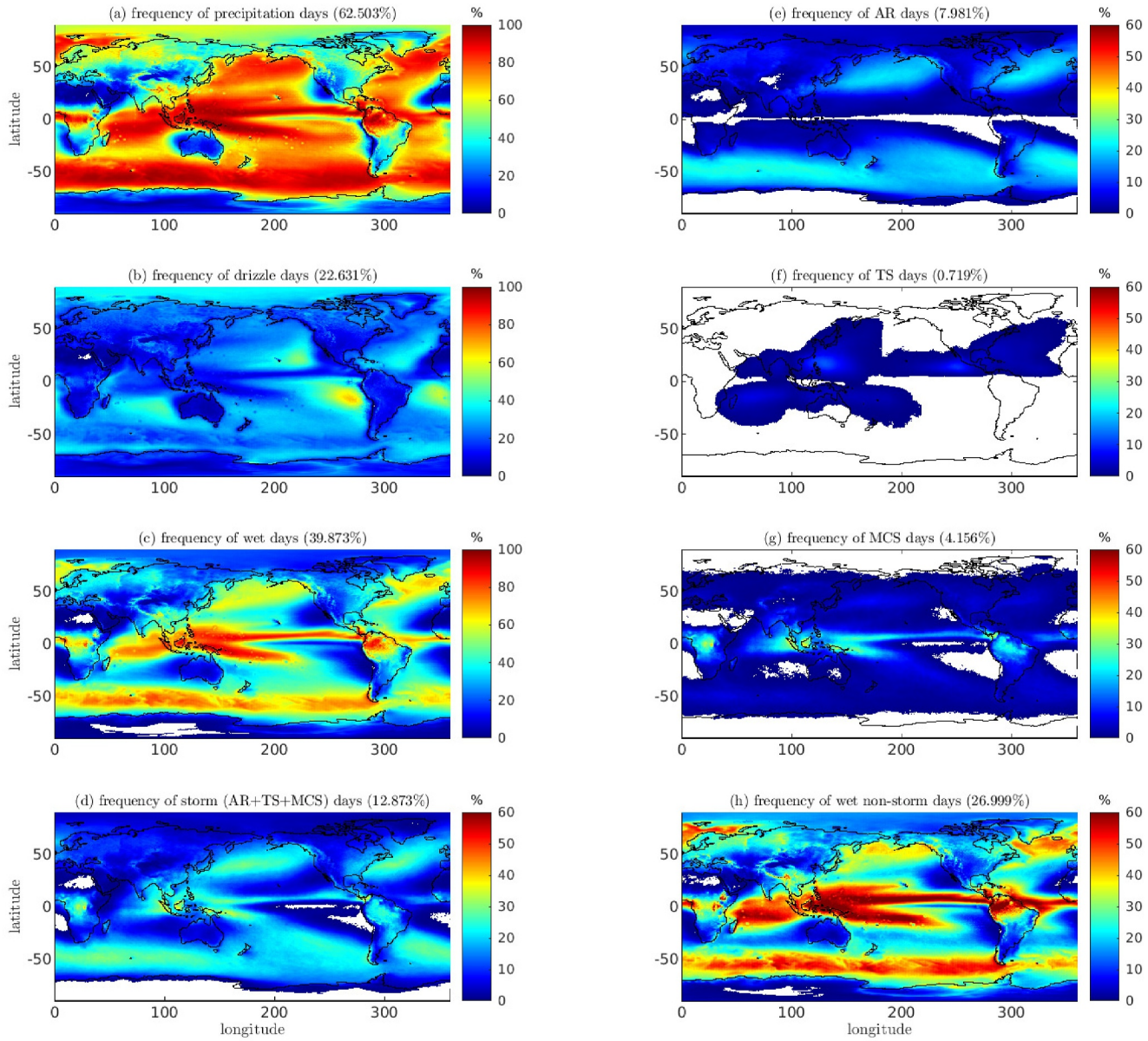

Figure 1. Geographical distribution of annual occurrence frequency (unit: %) of (a) precipitation, (b) drizzle, (c) wet, (d) storm (i.e., AR + TS + MCS), (e) AR, (f) TS, (g) MCS, and (h) wet non-storm days derived from observations. The global area-weighted mean value is shown on the top of each panel. Note panel (c) is the sum of panels (d and h). Panel (d) is the sum of panels (e–g).

Globally, the frequency-weighted average of LW CRE from non-precipitation, drizzle, and wet non-storm days are 11.8, 18.6, and 33.1 W m^{-2}, respectively. In contrast, the frequency-weighted average of LW CRE from AR, TS, and MCS days is 49.1, 75.5, and 90.6 W m^{-2}, respectively. On average, the LW CRE from storm days is about twice as large as that from wet non-storm days, 3–4 times that from drizzle days, and 5–6 times that from non-precipitation days, which explains their disproportionately larger contribution to global and annual LW CRE. Additionally, there is significant spatial variation in the LW CRE associated with AR and TS days, with larger LW CRE typically occurring over warmer oceans. However, the spatial variation of LW CRE associated with MCS days is generally small in the tropics. This is likely due to the definition of MCS, which relies on a brightness temperature threshold corresponding to an OLR threshold.

We now depict the spatial distribution of the annual mean SW CRE and its contributions from drizzle, wet, AR, TS, MCS, storm, and wet non-storm days in Figure 3. The SW CRE associated with AR, TS, and MCS days

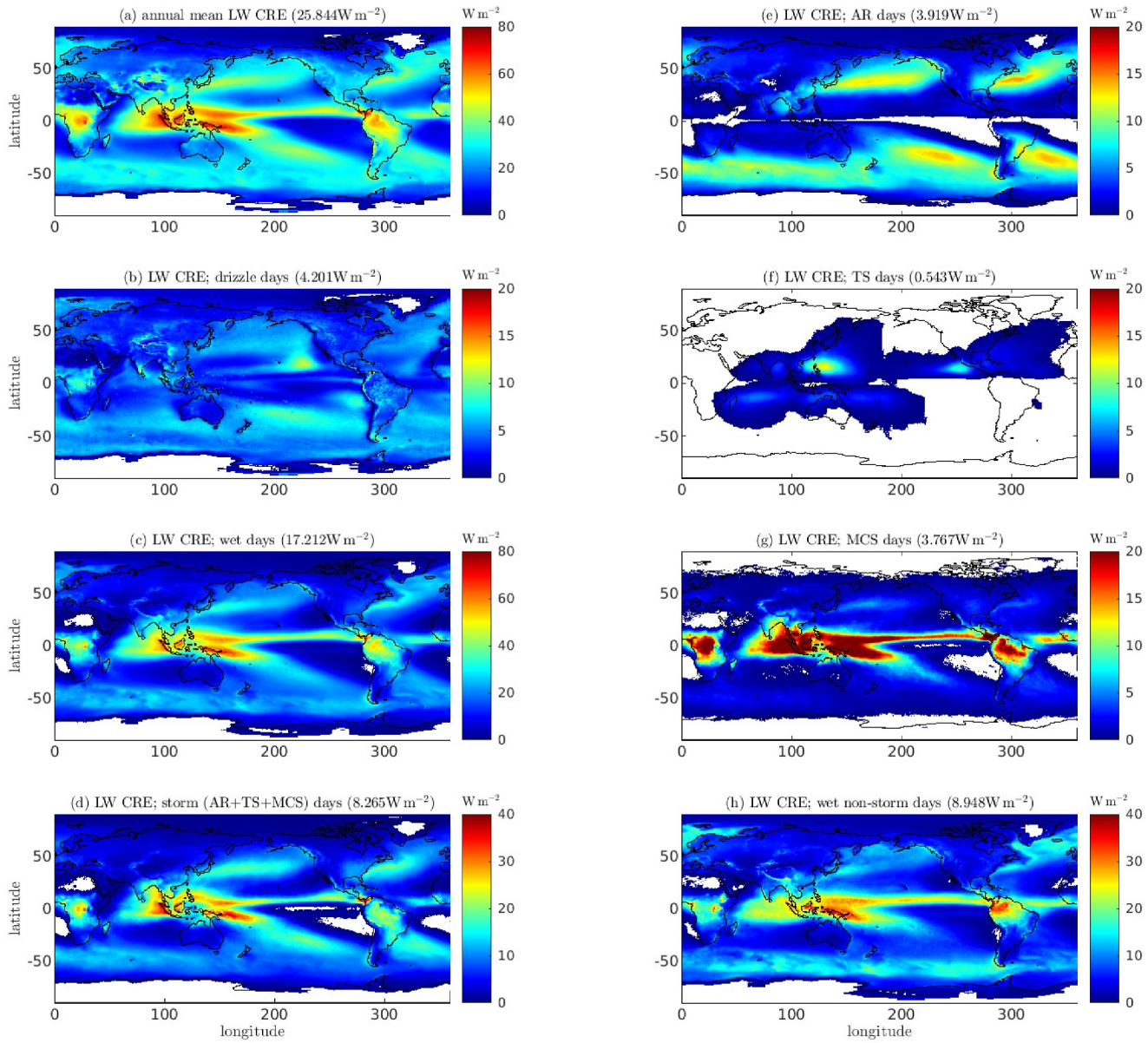

Figure 2. Geographical distribution of (a) annual mean LW CRE (unit: W m^{-2}) and its contributions from (b) drizzle, (c) wet, (d) storm (i.e., AR + TS + MCS), (e) AR, (f) TS, (g) MCS, and (h) wet non-storm days derived from observations. The contribution from each regime is computed as the accumulated LW CRE of that regime at any given grid cell, which depends on both the regime's occurrence frequency and its intensity in LW CRE. The global area-weighted mean value is shown on the top of each panel. Note panel (c) is the sum of panels (d and h). Panel (d) is the sum of panels (e–g).

together is roughly 27% (−12.2 W m^{-2}) of the global and annual mean SW CRE, which is also disproportionately larger in magnitude than their global frequency of occurrence. In comparison, the SW CRE associated with the wet non-storm days contributes roughly (33%) (−15.2 W m^{-2}). Thus, wet days account for a total of 60% of the global TOA SW CRE, which is smaller than their contribution to TOA LW CRE. Combined with drizzle days, the total precipitation days account for 82% of the global and annual SW CRE, which is only slightly smaller than their contribution to the global LW CRE (83%). Thus, precipitation days are important to both LW and SW CRE. Individually, the global and annual mean SW CRE associated with AR, TS, and MCS days are respectively −6.76 W m^{-2} (15%), −0.73 W m^{-2} (1.6%), and −4.65 W m^{-2} (10%). Regionally, the percentage contribution to SW CRE from AR, TS, and MCS days can also be substantially larger (40%–50%), especially over the ITCZ, the SPCZ, and the mid-latitude storm track regions, with AR and MCS days dominating the mid-latitudes and tropics, respectively. Taking together, the storm days contribute significantly to both SW and LW CRE around the globe,

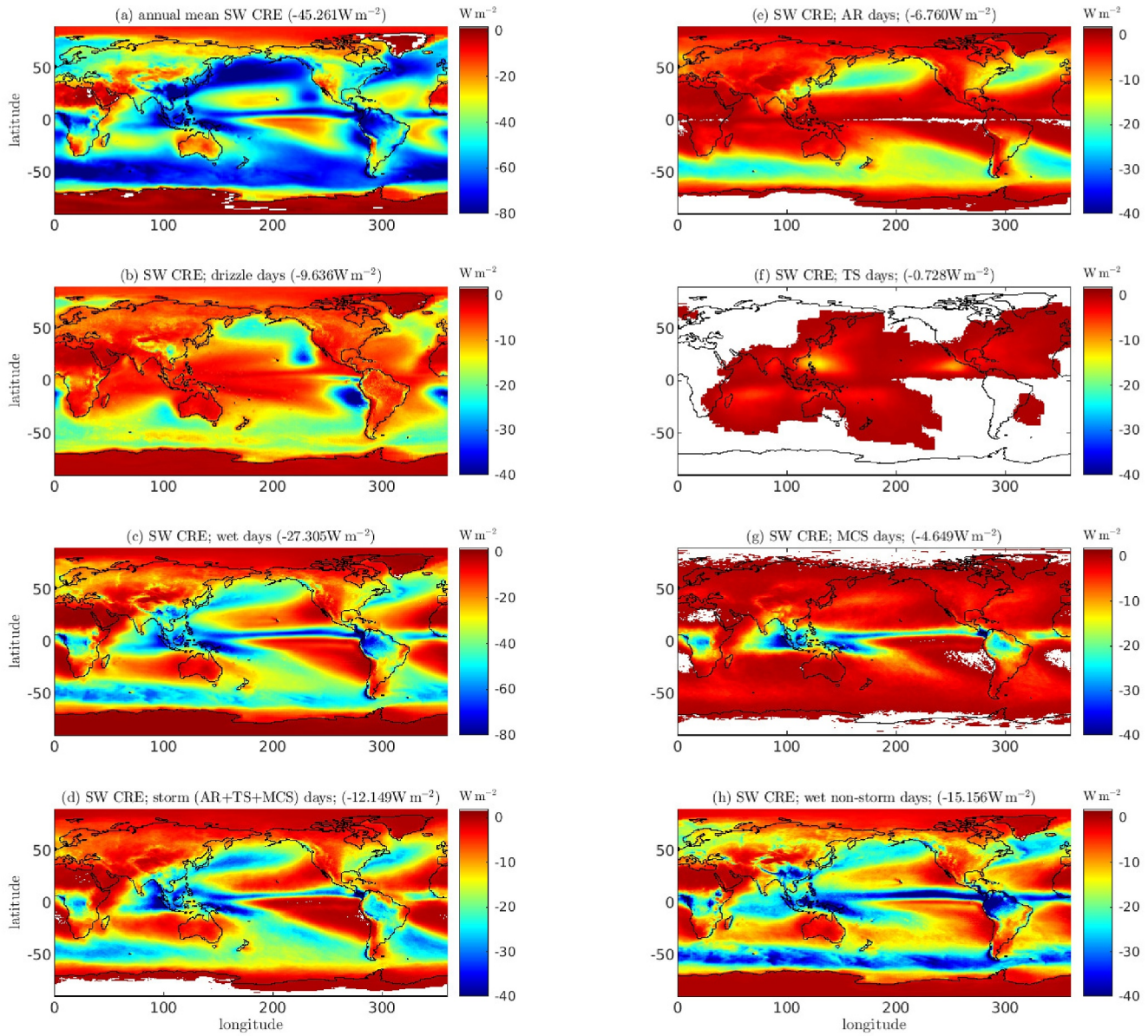

Figure 3. As in Figure 2 but for SW CRE.

except over the subsiding branch of the Hadley and Walker circulation and the high latitudes, roughly 60° poleward.

Figure S2 in Supporting Information S1 displays the geographical distribution of SW CRE averaged from non-precipitation, drizzle, wet, AR, TS, MCS, storm, and wet non-storm days. Comparing with Figure S1 in Supporting Information S1, we can see that the SW CRE associated with stratocumulus clouds along the west coast of North and South America, Africa, and Australia, as well as the stratus over high latitude oceans stands out as a much larger contributor to SW CRE than LW CRE despite producing little precipitation (Figures S2a and S2b in Supporting Information S1). In contrast, non-precipitation and drizzle days produce much less SW CRE over other regions. Globally, the frequency-weighted average of SW CRE from non-precipitation, drizzle, wet non-storm days are −22.2, −42.6, −56.1 W m^{-2}, respectively. In contrast, the frequency-weighted average of SW CRE from AR, TS, and MCS days is −84.7, −101.2, and −111.9 W m^{-2}, respectively. On average, the SW CRE from storm days is about 1.7 times as large as that from wet non-storm days, 2.2 times that from drizzle days, and

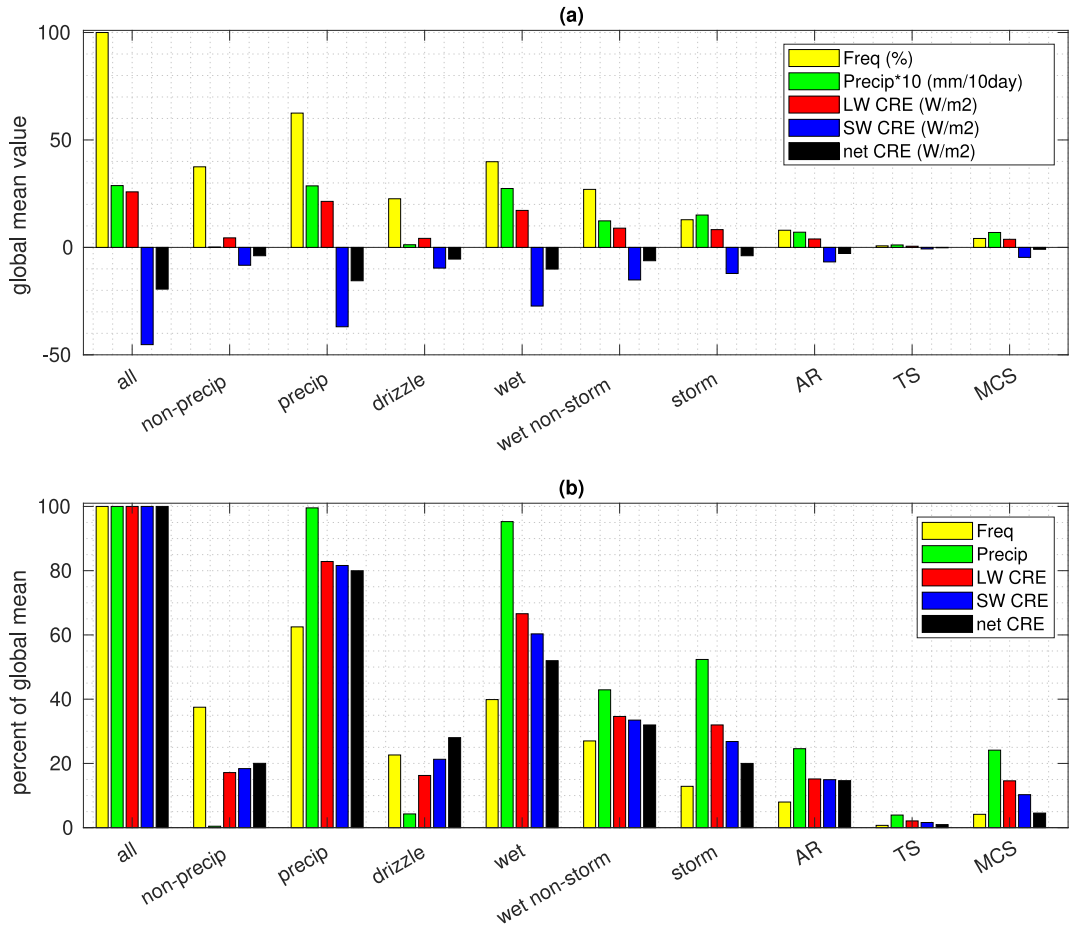

Figure 4. (a) Global and annual mean surface precipitation (unit: mm per 10 days, scaled up by a factor of 10 for plotting convenience), TOA LW, SW, and net CRE (unit: W m^{-2}), and their contributions from non-precipitation, precipitation, drizzle, wet, wet non-storm, storm, AR, TS, and MCS days. Yellow bars show the global occurrence frequency of each weather regime studied here. The global and annual mean values are denoted as "all." Note that, by definition, all = non-precip + precip; precip = drizzle + wet; wet = wet non-storm + storm; storm = AR + TS + MCS. (b) As in (a) but normalized by the global mean value of each variable to illustrate their percentage contribution to the global means (%).

4.3 times that from non-precipitation days, which explains their disproportionately larger contribution to global and annual SW CRE.

We summarize in Figure 4 the global frequency of daily precipitation regimes and their associated CRE, as well as precipitation. Table S1 in Supporting Information S1 provides the detailed numbers. The precipitation days account for roughly 80% of global LW, SW, and net CREs, despite their frequency being approximately 60%. When comparing drizzle and wet days, it becomes evident that wet days exert greater influence on LW, SW, and net CRE among the total precipitation days. This dominance stems from their higher frequency and intensity in CREs. Comparing storm and wet non-storm days, storm days produce nearly as large CREs as the wet non-storm days despite their frequency being only half of the wet non-storm days. This is especially true for LW CRE. Their disproportionately larger impact on CREs is due to their greater intensity in CREs. Among the storm days, the AR and MCS days dominate the total storm days, while TS days contribute minimally to the global CRE (1%–2%) due to their very low occurrence frequency. The global frequency of AR days is approximately 8% but their contribution to global LW and SW CRE amounts to about 15%. Similarly, the global frequency of MCS days is around 4%, but their contribution to global LW and SW CRE is approximately 15% and 10%, respectively. The net CRE associated with MCS days is substantially smaller than that from the AR days. This discrepancy arises because MCS days exhibit a larger compensation (in absolute values) between the LW and SW components (Figure 4a). However, since LW CRE primarily affects the atmosphere and SW CRE mainly impact the ocean and

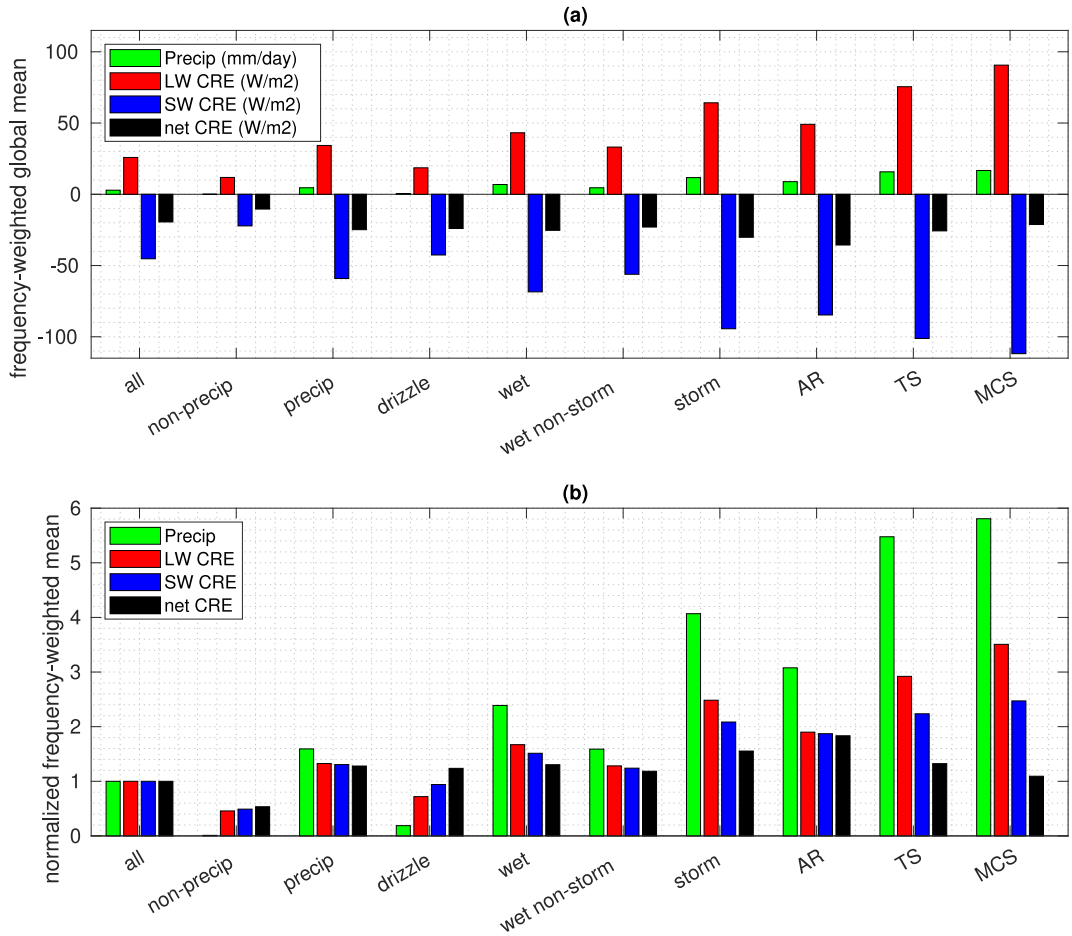

Figure 5. (a) Frequency-weighted global mean ($\left[\overline{\Phi_X}\right]$) precipitation (mm day^{-1}), TOA LW, SW, and net CRE (W m^{-2}) averaged across various weather regimes, including non-precipitation, precipitation, drizzle, wet, wet non-storm, storm, AR, TS, and MCS days. The global and annual mean values are denoted as "all." The expression $\left[\overline{\Phi_X}\right]$ is computed as follows: $\left[\overline{\Phi_X}\right] = \int_y\int_x \overline{\Phi_X}(x,y)F_X(x,y)dx\,dy / \int_y\int_x F_X(x,y)dx\,dy$. Here X represents non-precipitation, precipitation, drizzle, wet, wet non-storm, storm, AR, TS, and MCS days, $\overline{\Phi_X}$ denotes the mean quantity averaged over all X days at each location (x, y), and F_X denotes the occurrence frequency of X days at (x, y). (b) As in (a), but normalized by the corresponding global mean value of each variable to show their intensity relative to the global annual mean.

land surface, their influence on weather and climate needs to be separately considered in the ocean-atmosphere and land-coupled Earth system.

Finally, we summarize in Figure 5 the frequency-weighted global mean intensities in CRE and precipitation averaged from each weather regime. Table S2 in Supporting Information S1 provides the detailed numbers. On average, precipitation days produce 2–3 times larger LW and SW CRE than non-precipitation day. Wet days generate 2.3 times larger LW CRE and 1.6 times larger SW CRE larger than that of drizzle days. However, the two components tend to cancel each other out to some extent, leaving a smaller difference in the intensity of net CRE. Storm days produce nearly twice as large LW CRE and 1.7 times larger SW CRE than wet non-storm days. TS and MCS days produce significantly larger LW and SW CRE than AR days. However, the two components tend to cancel to a larger extent and thus result in a smaller net CRE than the AR days.

4. Summary

We have utilized high temporal resolution satellite observations, reanalysis data, observed TS tracks, and surface precipitation data to quantify, for the first time, the global number and regional distribution of LW, SW, and net CRE associated with AR, TS, and MCS. In doing so, we have also examined other distinct daily weather regimes

such as wet non-storm, drizzle, and non-precipitation days based on daily precipitation rates. While previous studies tend to emphasize fair-weather cumuli and stratocumulus clouds, which usually exhibit little surface precipitation but extensive spatial coverage (shallow cumuli) or strong net CRE (stratocumulus), our focus here is on high-impact storm systems such as AR, TS, and MCS. These events, often associated with extreme precipitation, strong winds, and local disasters, are typically considered rare events. Our findings reveal that despite their rarity (13% globally), these events significantly contribute (32% and 27%) to global LW and SW CRE. These figures are nearly equivalent to those from wet non-storm days. Moreover, the wet days collectively contribute approximately 67% and 60% to the global LW and SW CRE, respectively. When combined with drizzle days, total precipitation days contribute 83% and 82% to global LW and SW CRE, respectively. Thus, various precipitation weather regimes, including storms, are essential for regulating Earth's radiation budget. It is important to note that our study quantifies only the direct CRE associate with storms. However, these storms can also have indirect effect on CRE over remote regions by inducing large-scale circulation and transporting water vapor and heat. Quantifying these impacts, however, is more challenging.

The present study is important not only for better quantifying and understanding the roles of various weather systems in the TOA radiation budget but also for evaluating climate models. Climate model development often tunes present-day CRE to match observed long-term mean climatology. However, models with similar climatological CRE can exhibit significant differences due to compensating errors across various weather regimes. These discrepancies among weather regimes in climate models could lead to diverse cloud feedback as weather patterns evolve in a warmer climate. Hence, it is imperative to incorporate additional observational constraints on modeled CREs specific to individual weather regimes. Our study serves as an example of this endeavor. Furthermore, given the large contribution of precipitating clouds to Earth's TOA radiation budget, as demonstrated here, accurately modeling precipitation processes in climate models is crucial. However, representing precipitation in climate models remains challenging and must be parameterized due to coarse model resolution and long time-steps. The analysis based on precipitation weather regimes presented here offers additional avenues to constrain modeled CRE and precipitation at the process level.

Data Availability Statement

The synoptic TOA and surface fluxes and clouds data set (SYN1deg-Ed4.1 Level 3) from Clouds and the Earth's Radiant Energy System (CERES) are available at https://ceres.larc.nasa.gov/data/. The Multi-Source Weighted-Ensemble Precipitation (MSWEP-v2) data set is available at https://www.gloh2o.org/mswep/. The integrated vapor transport (IVT) data from ERA-5 reanalysis are available at https://www.ecmwf.int/en/forecasts/dataset/ecmwf-reanalysis-v5. The International Best Track Archive for Climate Stewardship (IBTrACS) data are available at https://www.ncei.noaa.gov/products/international-best-track-archive. The CLoud Archive User Service (CLAUS) multisatellite infrared brightness temperature data set is available at https://data.ceda.ac.uk/badc/claus/data.

Acknowledgments
We thank Drs. Leo Donner, Ryan Kramer, and the two anomalous reviewers for their comments and suggestions. The statements, findings, conclusions, and recommendations are those of the authors and do not necessarily reflect the views of the National Oceanic and Atmospheric Administration or the US Department of Commerce.

References

Beck, H. E., Wood, E. F., Pan, M., Fisher, C. K., Miralles, D. M., van Dijk, A. I. J. M., et al. (2019). MSWEP V2 global 3-hourly 0.1° precipitation: Methodology and quantitative assessment. *Bulletin of the American Meteorological Society*, *3*, 473–500. https://doi.org/10.1175/bams-d-17-0138.1

Bony, S., & Dufresne, J.-L. (2005). Marine boundary layer clouds at the heart of tropical cloud feedback uncertainties in climate models. *Geophysical Research Letters*, *32*(20), L20806. https://doi.org/10.1029/2005GL023851

Bony, S., Dufresne, J.-L., Treut, H. L., Morcrette, J.-J., & Senior, C. (2004). On dynamic and thermodynamic components of cloud changes. *Climate Dynamics*, *22*(2–3), 71–86. https://doi.org/10.1007/s00382-003-0369-6

Bretherton, C. S. (2015). Insights into low-latitude cloud feedbacks from high-resolution models. *Philosophical Transactions of the Royal Society A*, *373*(2054), 20140415. https://doi.org/10.1098/rsta.2014.0415

Cess, R., Potter, G., Blanchet, J. P., Boer, G. J., Del Genio, A. D., Déqué, M., et al. (1990). Intercomparison and interpretation of climate feedback processes in 19 atmospheric general circulation models. *Journal of Geophysical Research*, *95*(D10), 16601–16615. https://doi.org/10.1029/jd095id10p16601

Danabasoglu, G., Lamarque, J., Bacmeister, J., Bailey, D. A., DuVivier, A. K., Edwards, J., et al. (2020). The community earth system model version 2 (CESM2). *Journal of Advances in Modeling Earth Systems*, *12*(2), e2019MS001916. https://doi.org/10.1029/2019MS001916

Dong, W., Zhao, M., Ming, Y., & Ramaswamy, V. (2021). Representation of tropical mesoscale convective systems in a general circulation model: Climatology and response to global warming. *Journal of Climate*, *34*, 5657–5671. https://doi.org/10.1175/JCLI-D-20-0535.1

Donner, L. J., Wyman, B. L., Hemler, R., Horowitz, L. W., Ming, Y., and, M. Z., et al. (2011). The dynamical core, physical parameterizations, and basic simulation characteristics of the atmospheric component AM3 of the GFDL global coupled model CM3. *Journal of Climate*, *24*(13), 3484–3519. https://doi.org/10.1175/2011jcli3955.1

Flato, G., Marotzke, J., Abiodun, B., Braconnot, P., Chou, S. C., & Collins, W. (2013). Evaluation of climate models. In T. F. Stocker, D. Qin, G.-K. Plattner, M. Tignor, S. K. Allen, J. Boschung, et al. (Eds.), *Climate change 2013: The physical science basis. Contribution of Working Group I to the Fifth Assessment Report of the Intergovenmental Panel on Climate Change* (pp. 741–866). Cambridge University Press.

Golaz, J.-C., Caldwell, P. M., Roekel, L. P. V., Petersen, M. R., Tang, Q., Wolfe, J. D., et al. (2019). The DOE E3SM coupled model version 1: Overview and evaluation at standard resolution. *Journal of Advances in Modeling Earth Systems*, *11*(7), 2089–2129. https://doi.org/10.1029/2018MS001603

Guan, B., & Waliser, D. E. (2015). Detection of atmospheric rivers: Evaluation and application of an algorithm for global studies. *Journal of Advances in Modeling Earth Systems*, *120*(24), 12514–12535. https://doi.org/10.1002/2015JD024257

Held, I. M., Guo, H., Adcroft, A., Dunne, J. P., Horowitz, L. W., Krasting, J., et al. (2019). Structure and performance of GFDL's CM4.0 climate model. *Journal of Advances in Modeling Earth Systems*, *11*(11), 3691–3727. https://doi.org/10.1029/2019MS001829

Hersbach, H., Bell, B., Berrisford, P., Hirahara, S., Horányi, A., Muñoz-Sabater, J., et al. (2020). The ERA5 global reanalysis. *Quarterly Journal of the Royal Meteorological Society*, *146*(730), 1999–2049. https://doi.org/10.1002/qj.3803

Hodges, K. I., Chappell, D. W., Robinson, G. J., & Yang, G. (2000). An improved algorithm for generating global window brightness temperatures from multiple satellite infrared imagery. *Journal of Atmospheric and Oceanic Technology*, *17*(10), 1296–1312. https://doi.org/10.1175/1520-0426(2000)017<1296:aiafgg>2.0.co;2

Knapp, K. R., Kruk, M. C., Levinson, D. H., Diamond, H. J., & Neumann, C. J. (2010). The International Best Track Archive for Climate Stewardship (IBTrACS) - Unifying tropical cyclone best track data. *Bulletin America Meteorology Social*, *91*(3), 363–376. https://doi.org/10.1175/2009bams2755.1

Loeb, N. G., Wielicki, B. A., Doellingast, D. R., Smith, G. L., Keyes, D. F., Kato, S., et al. (2009). Toward optimal closure of the Earth's top-of-atmosphere radiation budget. *Journal of Climate*, *22*(3), 748–766. https://doi.org/10.1175/2008JCLI2637.1

Meehl, G. A., Stocker, T. F., Collins, W. D., Friedlingstein, P., Gaye, A. T., Gregory, J. M., et al. (2007). Global climate projection. In S. Solomon, D. Qin, M. Manning, Z. Chen, M. Marquis, K. B. Averyt, et al. (Eds.), *Climate change 2007: The physical science basis. Contribution of Working Group I to the Fourth Assessment Report of the intergovenmental Panel on Climate Change* (pp. 589–662). Cambridge University Press.

Oreopoulos, L., Cho, N., Lee, D., & Kato, S. (2016). Radiative effects of global MODIS cloud regimes. *Journal of Geophysical Research*, *121*(5), 2299–2317. https://doi.org/10.1002/2015jd024502

Randall, D., Wood, R., Bony, S., Colman, R., Fichefet, T., Fyfe, J., et al. (2007). Climate models and their evaluation. In S. Solomon, D. Qin, M. Manning, Z. Chen, M. Marquis, K. B. Averyt, et al. (Eds.), *Climate change 2007: The physical science basis. Contribution of Working Group I to the Fourth Assessment Report of the Intergovenmental Panel On Climate Change* (pp. 589–662). Cambridge University Press.

Smith, G. L., Priestley, K. J., Loeb, N. G., Wielicki, B. A., Charlock, T. P., Minnis, P., et al. (2011). Clouds and Earth radiant Energy system (CERES), a review: Past, present and future. *Advances in Space Research*, *48*(2), 254–263. https://doi.org/10.1016/j.asr.2011.03.009

Soden, B., & Held, I. (2006). An assessment of climate feedbacks in coupled ocean-atmosphere models. *Journal of Climate*, *19*(14), 3354–3360. https://doi.org/10.1175/jcli3799.1

Yuan, T., Oreopoulos, L., Platnick, S. E., & Meyer, K. (2018). Observations of local positive low cloud feedback patterns and their role in internal variability and climate sensitivity. *Geophysical Research Letters*, *45*(9), 4438–4445. https://doi.org/10.1029/2018GL077904

Zhao, M. (2014). An investigation of the connections among convection, clouds, and climate sensitivity in a global climate model. *Journal of Climate*, *27*(5), 1845–1862. https://doi.org/10.1175/jcli-d-13-00145.1

Zhao, M. (2020). Simulations of atmospheric rivers, their variability, and response to global warming using GFDL's new high-resolution general circulation model. *Journal of Climate*, *33*(23), 10287–10303. https://doi.org/10.1175/JCLI-D-20-0241.1

Zhao, M. (2022a). An investigation of the effective climate sensitivity in GFDL's new climate models CM4.0 and SPEAR. *Journal of Climate*, *35*(17), 5637–5660. https://doi.org/10.1175/JCLI-D-21-0327

Zhao, M. (2022b). A study of AR-TS-and MCS-associated precipitation and extreme precipitation in present and warmer climates. *Journal of Climate*, *35*(2), 479–497. https://doi.org/10.1175/JCLI-D-21-0145.1

Zhao, M., Golaz, J.-C., Held, I., Ramaswamy, V., Lin, S.-J., Ming, Y., et al. (2016). Uncertainty in model climate sensitivity traced to representations of cumulus precipitation microphysics. *Journal of Climate*, *29*(2), 543–560. https://doi.org/10.1175/jcli-d-15-0191.1

Zhao, M., Golaz, J. C., Held, I. M., Guo, H., Balaji, V., Benson, R., et al. (2018). The GFDL global atmosphere and land model AM4.0/LM4.0 – Part II: Model description, sensitivity studies, and tuning strategies. *Journal of Advances in Modeling Earth Systems*, *10*(3), 735–769. https://doi.org/10.1002/2017MS001209

Zhao, M., Held, I. M., Lin, S.-J., & Vecchi, G. A. (2009). Simulations of global hurricane climatology, interannual variability, and response to global warming using a 50 km resolution GCM. *Journal of Climate*, *22*(24), 6653–6678. https://doi.org/10.1175/2009jcli3049.1